JACS
JOURNAL OF THE AMERICAN CHEMICAL SOCIETY
Article
pubs.acs.org/JACS

Topology-Driven Reductive Silylation of Synthetic Carbon Allotropes

Kathrin C. Knirsch, Ferdinand Hof, Vicent Lloret, Udo Mundloch, Frank Hauke, and Andreas Hirsch*

Department of Chemistry and Pharmacy & Joint Institute of Advanced Materials and Processes (ZMP), Friedrich-Alexander-University Erlangen-Nürnberg, Henkestraße 42, 91054 Erlangen, Germany

Supporting Information

ABSTRACT: Herein, the combined application of characterization tools, such as Raman spectroscopy, thermal gravimetric analysis coupled with mass spectrometry, and optical and atomic force microscopy, confirms the reductive silylation of synthetic carbon allotropes as a new covalent functionalization strategy for the formation of heteroatom−carbon bonds. In particular, our study gives interesting insights into the topology-driven retrofunctionalization of nanotubide and graphenide derivatives.

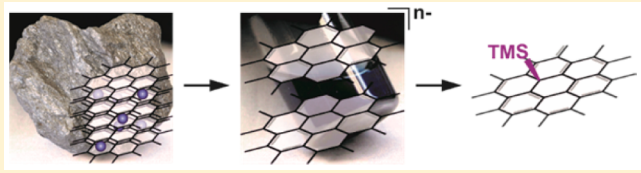

INTRODUCTION

The covalent functionalization of synthetic carbon allotropes (SCAs), such as carbon nanotubes (CNTs) and graphene, has fundamentally been progressed within the past decade.[1,2] Nevertheless, almost any SCA-based functionalization protocol draws on the covalent binding of functional entities via the formation of new carbon−carbon bonds. The direct attachment of heteroatoms to the carbon allotrope framework has only been described occasionally, and examples for silylation reactions are extremely rare.[3−5] This is in stark contrast to the classical organic chemistry, where silylation reactions represent a very versatile and most commonly used tool. Here, organosilanes serve, inter alia, as selective protecting groups, derivatization and reducing reagents, and cross-coupling compounds.[6]

In the field of SCA chemistry, the formation of organosilanes has so far been addressed only marginally, at best. This is a little bit surprising, as it has been shown by theory that silyl ($-SiH_3$) radicals form strong covalent bonds with graphene and nanotube sidewalls.[3] In their survey of various substituents on single-walled carbon nanotubes (SWCNTs), introduced via an electron transfer mediating reagent, Maeda et al. briefly mentioned the attachment of trimethylsilyl and triethylsilyl functionalities, solely based on a Raman spectroscopic sample analysis.[5] We have recently shown that reductive SCA functionalization protocols require strict control of the respective reaction conditions and that they are accompanied by the formation of side products.[7] Therefore, a reliable product characterization has to been founded on statistical Raman analysis[8−10] in combination with the data obtained by thermal gravimetric analysis coupled with mass spectrometry.[11]

In principle, the successful synthesis of organosilane-functionalized SCAs provides a perfect opportunity to fine-tune their electronic and physical properties due to the covalently bonded, electron-pushing trialkylsilyl group.

In the present report, we introduce a novel and versatile reductive silylation reaction for graphene and carbon nanotubes, which is based on a three-step protocol (Scheme 1), starting from the respective pristine allotrope. After the initial solid-state reduction via potassium as electron donor component and the subsequent ultrasonication-mediated exfoliation of the respective intercalated species in an inert solvent, silylating reagents, e.g. trimethylsilyl chloride (TMS-Cl), were added as trapping reagents to the respective graphenide/carbon nanotubide dispersion.

Scheme 1. Reductive Exfoliation of SCAs and Subsequent Trapping of Intermediately Generated Graphenides/Carbon Nanotubides with Trimethylsilyl Chloride[a]

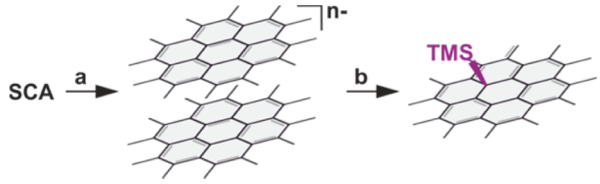

[a]All reactions were carried out inside the glovebox. Legend: (a) formation of reduced SCA starting materials: (1) potassium, 200 °C, 12 h; exfoliation: (2) inert solvent, tip sonication; (b) addition of silylating reagent TMS-Cl.

This novel functionalization sequence offers the possibility to strictly control the reaction conditions and to carry out an in-depth analysis of the intermediately formed SCA derivatives even prior to the aqueous workup of the bulk material. By means of statistical Raman spectroscopy (SRS), mass spectrometry coupled with thermal gravimetric analysis (TGA/MS), and optical and atomic force microscopy (AFM), we were able to show that a successful reductive silylation of SCAs is possible and that the stability of the attached trialkylsilyl moieties drastically depends on the reaction and workup conditions. Furthermore, data obtained for the reductive silylation of graphene were directly compared with the established reductive arylation protocol[9] and the influence of the size of the alkyl chain was investigated. Most interestingly, by the direct comparison of the

Received: September 9, 2016
Published: November 2, 2016

DOI: 10.1021/jacs.6b09487
J. Am. Chem. Soc. 2016, 138, 15642−15647

reductive silylation of graphene vs CNTs we found a topological-based reversibility of the functionalization in the case of the one-dimensional (1D) carbon allotrope. Here, an initially formed kinetic addition product is transferred into the respective thermodynamically stable system.

RESULTS AND DISCUSSION

In order to gain a detailed insight into the reductive silylation of SCAs and to confirm that a successful addition of a silyl moiety to the sp^2 carbon scaffold is possible, we first concentrated on an in situ analysis of the functionalization of graphenides[12] under strict inert gas conditions (Scheme 1) in analogy to the study carried out by Hof et al.[7]

For the generation of the individualized, charged, and highly reactive graphene intermediates, we used as a precursor compound the respective graphite intercalation compound (GIC)[13−15] formed by melting potassium with a spherical graphite[16] at 200 °C under an argon atmosphere (glovebox; <0.1 ppm oxygen, <0.1 ppm water) overnight. This bronze-colored salt was dispersed in dry and oxygen-free 1,2-dimethoxyethane (DME) mediated by short ultrasonication, to obtain the solvent-driven individualization of the reduced graphene layers (see the Supporting Information for detailed sample preparation). It has to be kept in mind that strictly H_2O- and O_2-free solvents are mandatory for the successful reductive exfoliation and in order to suppress side reactions during the functionalization.[7] Furthermore, the solvent has to be stable against the respective reduced SCA, which is nicely demonstrated for DME, as the bronze-colored intercalation compound disperses with the simultaneous formation of a blue alkalide/free electron solution (Figure 1).[17] After sedimentation for a few minutes, the bronze

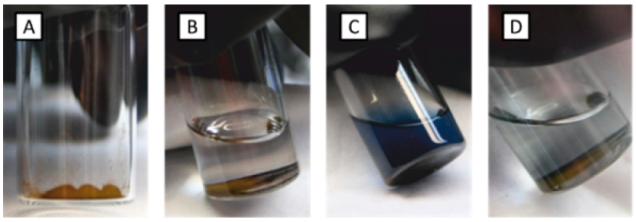

Figure 1. (A) Bronze-colored potassium GIC bulk material. (B) GIC in DME. (C) Exfoliation of GIC in DME by stirring, generating a blue alkalide/free electron solution. (D) Fully reversible precipitation of dispersed material.

color of the GIC reappeared while the inert solvent became colorless again (see also Figure S1 in the Supporting Information).

For the in situ monitoring of the reductive silylation reaction, TMS-Cl was added to the graphenide dispersion and the reaction mixture was stirred for 3 days. Raman sample preparation (TMS-$[G]_{inert}$) was conducted inside the glovebox. The functionalized product was filtered, and the obtained film (graphenopaper)[16] was hermetically sealed between two glass slides. SRS represents a quantitative and reliable analytical tool (Figure S2 in the Supporting Information) for the bulk characterization of covalently functionalized carbon nanomaterials.[8−10] In general, the Raman spectrum of graphene exhibits three main peaks—the defect induced D band at 1350 cm^{-1}, the G band at 1582 cm^{-1}, which is characteristic for the graphitic sp^2 carbon lattice, and the 2D band at 2700 cm^{-1} providing information about the stacking or electronic decoupling of the graphene layers.[18,19] The amount of sp^3 carbon atoms of the basal plane, bearing a covalently bound entity, correlates with the I_D/I_G intensity ratio and therefore corresponds to the degree of functionalization. In combination with the frequency distribution of the individual I_D/I_G values (Figure 2, left column),

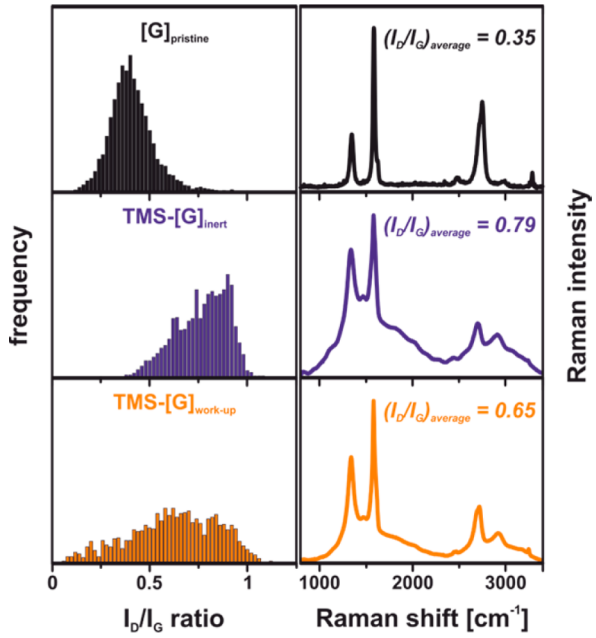

Figure 2. (left) Raman histograms (I_D/I_G ratio distribution) of the graphite starting material $[G]_{pristine}$ (black) and the TMS-functionalized reaction product TMS-$[G]_{inert}$ obtained after 3 days of stirring (blue)—kept under inert gas atmosphere—and after aqueous workup TMS-$[G]_{workup}$ (orange), measured under ambient conditions. (right) Averaged spectra of the respective samples, $\lambda_{exc.}$ 532 nm.

which is a measure for the sample homogeneity, the averaged Raman spectra (Figure 2, right column) can be taken as a representative description of the respective bulk material.

After the addition of TMS-Cl as trapping electrophile for the intermediately formed graphenides, a pronounced increase of the $(I_D/I_G)_{average}$ value (Figure 2, middle) with respect to the pristine starting material (0.35) (Figure 2, top) can be observed. Here, for TMS-$[G]_{inert}$ one broad I_D/I_G ratio distribution with an $(I_D/I_G)_{average}$ value of 0.79 is obtained. This I_D/I_G value increase of the primary reaction product is indicative of a successful reductive addition of trimethylsilyl groups to the graphene sp^2 framework and the formation of a covalent Si−C(sp^3) bond. The final degree of functionalization also depends on the dispersion efficiency of the solvent used for the stabilization of the exfoliated graphenide flakes. In principle, the reductive silylation can be carried out directly, without any solvent, just by the use of the liquid electrophilic trapping reagent TMS-Cl (Scheme S1 in the Supporting Information). Here, the Raman spectroscopically determined degree of functionalization is about 26% lower than that in the case of the DME-based functionalization sequence (Figure S3 in the Supporting Information). This could be explained by a less potent exfoliation/dispersion efficiency of TMS-Cl with respect to the intermediately generated graphenide flakes. Their fast aggregation leads to a reduction of the accessible surface area and finally to the reduced degree of functionalization. As in the case of reductive functionalization reactions with alkyl/aryl halides,[9,20] the formation of an activated graphite species (GIC) is another fundamental prerequisite for the successful attachment

DOI: 10.1021/jacs.6b09487
J. Am. Chem. Soc. 2016, 138, 15642−15647

of silyl moieties to the graphene basal plane. To illustrate this fact, a reference experiment was carried out where pristine graphite was used as starting material without an initial reductive activation (Scheme S2 in the Supporting Information). Here, no increase of the Raman $(I_D/I_G)_{average}$ value was detected (Figure S4 in the Supporting Information). This observation (see also Figures S5 and S6 in the Supporting Information) leads to the conclusion that the negatively charged graphenide intermediates act as electron donor components which initiate the formation of TMS radicals. Subsequently, the silicon-centered radicals attack the carbon allotrope sp^2 system and are covalently bound via a Si−C(sp^3) bond. This radical-based mechanism represents the connecting link of the reductive silylation to analogous reductive graphene functionalization sequences.[21−25]

In addition to Raman spectroscopy, TGA/MS yields valuable information on the successful covalent attachment of TMS moieties. Here, the functionalized sample is continuously heated to only plotted to 600 °C due to the measurement of Ph-[G]i; ESI: silylated samples, in general, heated to 700 °C and the detached functional entities are detected by an EI mass spectrometer. For the reductively silylated sample a total mass loss of Δw_t = 8.3% is obtained over the whole temperature regime (Figure 3, left). This total mass loss is attributed to the detachment

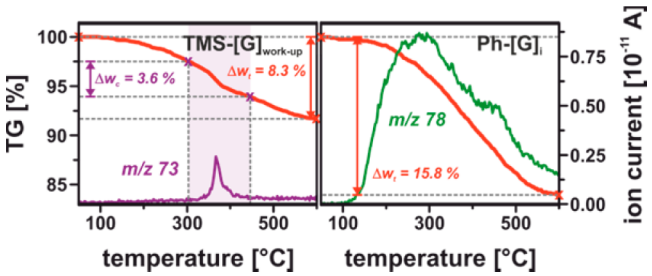

Figure 3. TGA-mass loss and ion current traces for (left) reductively silylated TMS-$[G]_{workup}$ and (right) reductively arylated Ph-$[G]_i$.

of volatile, noncovalently adsorbed entities and to the cleavage of functional groups at elevated temperatures. Therefore, for the calculation of the degree of functionalization only a corrected mass loss of Δw_c = 3.6%, which is assigned to the temperature region where the characteristic trimethylsilyl fragment (m/z 73) is detected, can be taken into account. On the basis of this fact, a degree of functionalization of 0.7% is determined for the reductive addition of the trimethylsilyl groups on graphene.

This value can directly be compared to the well-established reductive exfoliation/arylation[9] of graphite (Figure 3, right)−C−C(sp^3) bond formation. Here, a mass loss of 15.8% is measured and this translates into a degree of functionalization of 2.9%. The drastically reduced degree of functionalization in the case of the reductive silylation sequence can partially be explained by a cleavage of the covalently attached TMS moieties under the acidic aqueous workup conditions−reference experiments to clarify this observation have been carried out (see the Supporting Information). This assumption is also confirmed by the data analysis of the respective Raman spectra of TMS-$[G]_{workup}$ depicted in Figure 2 (bottom). In the course of the aqueous workup the inhomogeneity of the sample is increased and $(I_D/I_G)_{average}$ drops to a value of 0.65. This is indicative of a partial desilylation reaction (cleavage of the respective Si−C(sp^3) bonds) under partial restoration of the conjugated sp^2 carbon framework structure of graphene.

For a direct comparison and evaluation of the stability of the respective C−C(sp^3) bonds in carbon group functionalized graphene derivatives, we used 4-trimethylsilylphenyl bromide (TMSPh-Br) for the reductive exfoliation/arylation of graphite under equal reaction/workup conditions (see the Supporting Information). The respective Raman data of TMSPh-[G] is presented in Figure 4. Here, the analysis of the in situ characterized

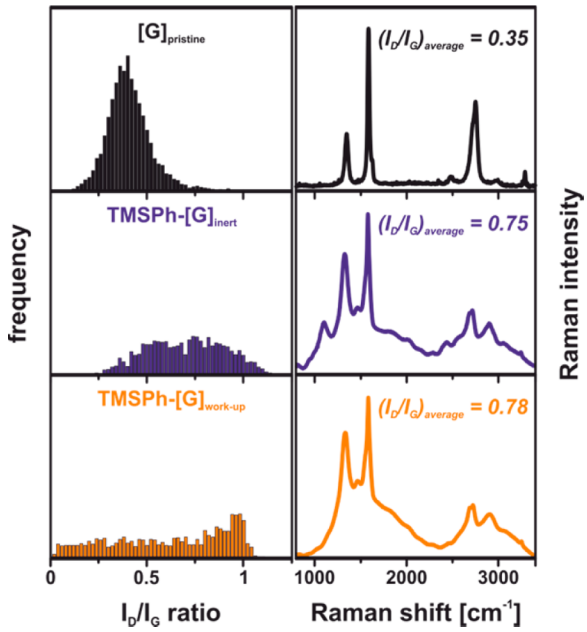

Figure 4. (left) Raman histograms (I_D/I_G ratio distribution) of the graphite starting material $[G]_{pristine}$ (black), the TMSPh-functionalized reaction product TMSPh-$[G]_{inert}$ obtained after 3 days of stirring (blue)−kept under inert gas atmosphere−and after aqueous workup TMSPh-$[G]_{workup}$ (orange), measured under ambient conditions. (right) Averaged spectra of the respective samples, $\lambda_{exc.}$ 532 nm.

trapping product TMSPh-$[G]_{inert}$ yields a $(I_D/I_G)_{average}$ value of 0.75 (Figure 4, middle). This is close to the Raman-determined degree of functionalization obtained for the reductively silylated sample (0.79) (Figure 2, middle).

In contrast to the latter case, the aqueous workup of the reductively arylated sample did not lead to a decrease of the measured $(I_D/I_G)_{average}$ value and can be taken as a clear indication that C−C(sp^3) bonds, as expected, are impervious to hydrolysis. Moreover, the obtained slight increase of $(I_D/I_G)_{average}$ to 0.78 (Figure 4, bottom) leads to the conclusion that untrapped negative charges present in the partially arylated graphenides trigger additional covalent functionalization reactions in the course of the aqueous workup, a fact which has already been proven for reductively charged carbon nanotubes.[7] The same effect is confirmed for our reductively silylated graphene derivatives. When TMS-$[G]_{inert}$ (preparation under inert gas conditions) is exposed to ambient conditions (moisture/oxygen), an increase of the Raman-determined degree of functionalization is observed (Figure S13 in the Supporting Information). Again, this subsequent functionalization leads to the formation of mixed functionalized graphene derivatives, which can only be prevented if electron trapping reagents such as benzonitrile are used prior to the aqueous workup.[26]

The GIC-activated silylation of graphene represents a variable concept, as silyl chlorides with different chain lengths and branching can be used. In the case of the bulky trihexylsilyl chloride (THS-Cl), the final reaction product after

DOI: 10.1021/jacs.6b09487
J. Am. Chem. Soc. 2016, 138, 15642−15647

aqueous workup (THS-[G]; for sample characterization see Figures S14–S18 in the Supporting Information) exhibits an $(I_D/I_G)_{average}$ value of 0.92 (Figure S14), which is about 29% higher than the degree of addition obtained for the reductive silylation with the smaller TMS functionality. In addition to the standard characterization techniques applied for all other silyl-functionalized graphene derivatives, we applied SRS and scanning Raman microscopy (SRM) to an in situ prepared sample of dodecyldimethylsilyl-functionalized graphene (DDMS-[G]) (Figure 5). Here, after the addition of dodecyldimethylsilyl chloride (DDMS-Cl) a sample was deposited on a Si/SiO_2 wafer (300 nm SiO_2 layer) and analyzed in detail.

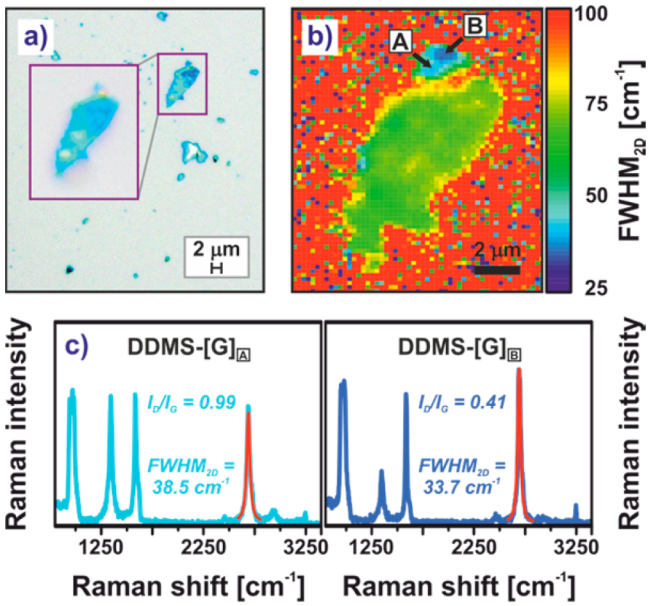

Figure 5. (a) Optical microscopy image of reductively silylated graphene (DDMS-[G]) flakes on a Si/SiO_2 wafer (300 nm SiO_2 layer). (b) SRM $FWHM_{2D}$ plot of the same flakes, which are highlighted in (a). (c) Representative single-point spectra of areas A and B, respectively. A Lorentz fit of the 2D band is shown in red.

In addition to some larger flakes (Figure 5a), the sample predominantly contained graphene flakes on the order of 2 μm. SRS/SRM analysis (Figure 5b,c and Figure S19 in the Supporting Information) showed that larger flakes with a full width at half-maximum of the 2D band ($FWHM_{2D}$) of around 60 cm^{-1} can be classified as covalently functionalized (I_D/I_G = 0.84) few-layer graphene. The $FWHM_{2D}$ values of the smaller flakes are in the range of 30–40 cm^{-1} and therefore clearly represent covalently silylated (I_D/I_G = 0.99) monolayer or bilayer graphene.[27]

For completeness, the Raman- and TGA/MS-based characterization of the bulk DDMS-[G] samples obtained under different workup conditions is summarized in Figures S7–S12 in the Supporting Information. In summary, all these results clearly prove that covalently silylated graphene is accessible by our reductive functionalization route, starting from activated graphite.

The potassium-based reductive silylation sequence can be variably transferred to the 1D carbon allotrope–SWCNTs. Here, for the reductive charging of HiPco SWCNTs (diameter range 0.8–1.2 nm) we followed the solid-state activation protocol–melting with potassium (for details see the Supporting Information).[28,29] The exfoliation of the carbon nanotubides was carried out in the well-suited dispersing solvent tetrahydrofuran (THF),[7] where side reactions can be excluded under inert gas conditions. As the reductive functionalization reagent, TMS-Cl was used, and the successful binding of the silyl moieties (TMS-[SWCNT]) was monitored by in situ Raman spectroscopic analysis (Figure S20 in the Supporting Information). In contrast to the study of Maeda et al.,[5] which was carried out via an electron transfer mediating reagent, we obtained a 2.3-fold higher degree of functionalization ($(I_D/I_G)_{average}$ value of 0.54, see Figure S20, bottom) after 3 days of reaction under inert gas conditions. This can most likely be attributed to the stronger reducing effect of potassium in comparison to Li/4,4′-di-*tert*-butylbiphenyl.

Most interestingly, a careful comparative analysis of our Raman data (Figure 6, left, and Figure S20 in the Supporting Information)

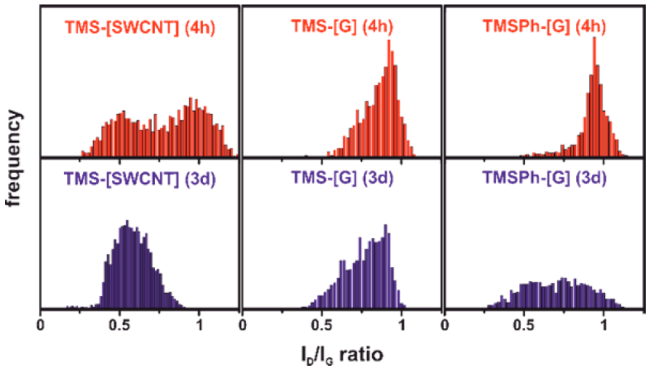

Figure 6. Raman histograms (I_D/I_G ratio distribution)–obtained under inert gas atmosphere. (left) Reductively silylated carbon nanotubides (TMS-[SWCNT]), with a bimodal product distribution after 4 hours and monomodal distribution after 3 days. (middle) Reductively silylated graphenides (TMS-[G]), with a monomodal distribution in both cases. (right) Reductively arylated graphenides (TMSPh-[G]), with a sharp monomodal distribution on the short time scale and broad distribution after 3 days.

revealed a time-dependent evolution of the degree of functionalization in the case of the reductive silylation of SWCNTs–a fact that has not been observed before.

On the short time scale (4 h reaction) the Raman histogram exhibits a bimodal distribution, indicative of the formation of two distinct main products with I_D/I_G values of around 0.5 and 1.0, respectively. After 3 days of stirring under inert gas conditions, only a monomodal distribution is obtained and the fraction with the higher degree of addition (I_D/I_G = 1.0) was converted into the product with a lower degree of functionalization. This observation can be explained by a topology-driven retrofunctionalization of the reductively silylated SWCNTs. Retrofunctionalization reactions of reductively alkylated carbon nanotube intermediates have already been observed,[30] but the time-resolved conversion of an addition product with a higher degree of functionalization into a final product with a lower degree of addition has not been described before.

From our perspective, this behavior can be attributed to the monotopic addition mechanism in the case of SWCNTs (functional groups can only be attached to one side of the carbon framework) and the subsequent increase of strain energy. It has to be anticipated that due to the large surface area of SWCNTs multiple, independent addend binding events take place. These initially bound addends serve as seeding spots for the binding of

DOI: 10.1021/jacs.6b09487
J. Am. Chem. Soc. 2016, 138, 15642–15647

additional entities in close vicinity. This spatial guidance of the first addend to distinct addition positions nearby is well documented for fullerenes.[31] Due to the nanotube curvature and the monotopic binding of a multitude of silyl groups in close proximity as well as on a relatively short time scale, the strain energy in these areas is increased. As a consequence, energy relaxation is achieved by a subsequent detachment of a part of the bound silyl entities (Figure 7)—by elimination

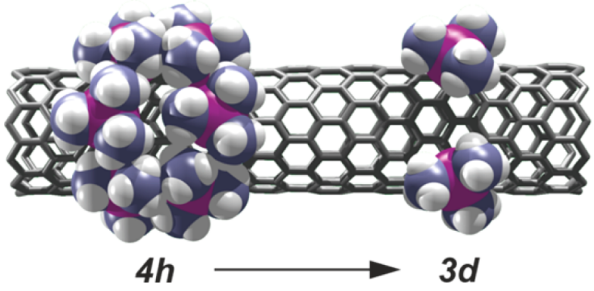

Figure 7. Reductively silylated carbon nanotubides. Initially bound addends can be detached from the nanotube sidewall within 3 days of reaction time as a result of the proven retrofunctionalization.

either of a silicon-centered radical (initial negative charging of the SWCNTs is preserved) or of a silyl anion (depletion of the initial negative charges in the nanotubide intermediates). Finally, after 3 days of reaction, an equilibrium configuration with a lower $(I_D/I_G)_{average}$ value of 0.54 in comparison to the $(I_D/I_G)_{average}$ value of 0.69, determined after 4 h of reaction time, is obtained.

Remarkably, the time-dependent evolution of the Raman histograms in the case of TMS-[G] (Figure 6, middle) only exhibits a monomodal distribution of the respective I_D/I_G values (centered at around 0.9) on the short (4 hours) and on the long time scales (3 days). This is easily explained by the fact that, in the case of the planar graphene, a ditopic binding of the addends (supratopic and antaratopic) is possible. In general, an addition of two substituents on opposite sides of the graphene basal planes prevents the buildup of local strain, even if a multitude of addition events occurs in a small, confined area. Therefore, no functional detachment is observed in the case of the reductive silylation of graphene. It has to be stated that in principle a retrofunctionalization may take place on a very short time scale (<3 h). However, this seems very unlikely, as in the case of graphene almost strain-free addition configurations—at least in the case of a moderate local addend density—are achieved by the supra- and antaratopic attack of the silyl radicals. In addition, this rationale is corroborated by the SRS data obtained for the reductive arylation of graphite (Figure 6, right). Here, as in the case of the reductively silylated SWCNT sample, a time-dependent evolution of the Raman histograms is detectable. For TMSPh-[G], one sharp monomodal distribution of the I_D/I_G values (I_D/I_G of the maximum at around 0.9) arises after 4 h of reaction time. After 3 days of stirring a broad, almost bimodal distribution is obtained for the carbon addend functionalized graphenides. Again, this is indicative of a time-dependent detachment of a part of the covalently bound entities. This retrofunctionalization of carbon-based addends has previously been reported by our group.[32] As described above, this retroreaction is not observed in the case of the reductively silylated samples. This may be explained by the stability of the leaving group—silicon-centered anion/radical vs carbon-centered. This may lead to the fact that in the case of the silylated graphene samples seeding areas with a locally very high degree of addition, and therefore partial strain, are preserved to a larger extent than in the case of the aryl-functionalized graphenides (Scheme 2 and Figure S21 in the Supporting Information).

Scheme 2. Time-Dependent Detachment of a Part of the Covalently Bound Entities in the Case of (a) TMS-Functionalized Nanotubides and (c) TMSPh-Functionalized Graphenides, with Equilibrium between Retrofunctionalization and Functionalization, and No Occuring Retrofunctionalization in the Case of (b) TMS-Functionalized Graphenides

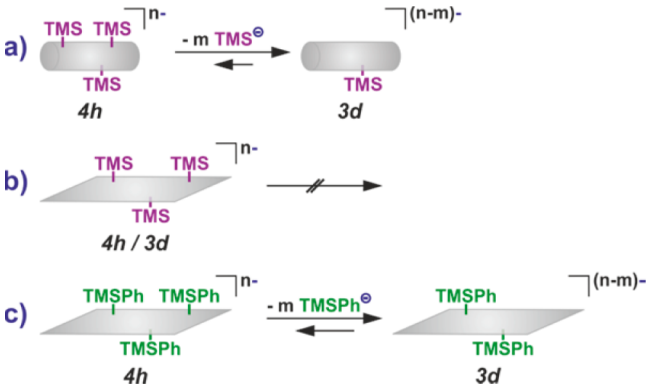

CONCLUSION

To summarize, a detailed analysis of the silyl-functionalized SCAs, namely carbon nanotubes and graphene, confirms the reductive silylation as a new and versatile covalent functionalization strategy achieving the direct attachment of a heteroatom to the carbon framework. A topology-driven retroreaction occurs in the course of the functionalization of nanotubides with TMS moieties. In contrast to the monotopic addend binding on nanotube sidewalls, an almost strain-free, ditopic addition reaction on graphenides only leads to a time-dependent retrofunctionalization when the stability of the leaving group is sufficient, which is perfectly in accordance with our previous reactivity studies.

ASSOCIATED CONTENT

Supporting Information

The Supporting Information is available free of charge on the ACS Publications website at DOI: 10.1021/jacs.6b09487.

Experimental procedures, additional Raman, TGA/MS, and microscopy data, and further information (PDF)

AUTHOR INFORMATION

Corresponding Author

*E-mail for A.H.: andreas.hirsch@fau.de.

Notes

The authors declare no competing financial interest.

ACKNOWLEDGMENTS

Dedicated to Prof. Hanack on the occasion of his 85th birthday. This work has been carried out within the framework of the SFB953 "Synthetic Carbon Allotropes". We thank the Graduate School Molecular Science (GSMS) for financial support. The

DOI: 10.1021/jacs.6b09487
J. Am. Chem. Soc. 2016, 138, 15642−15647

research leading to these results has received partial funding from the European Union Seventh Framework Programme under grant agreement no. 604391 Graphene Flagship.

REFERENCES

(1) Karousis, N.; Tagmatarchis, N.; Tasis, D. *Chem. Rev.* **2010**, *110*, 5366.
(2) Hirsch, A.; Englert, J. M.; Hauke, F. *Acc. Chem. Res.* **2013**, *46*, 87.
(3) Chang, K.; Berber, S.; Tománek, D. *Phys. Rev. Lett.* **2008**, *100*, 236102.
(4) Maeda, Y.; Sato, Y.; Kako, M.; Wakahara, T.; Akasaka, T.; Lu, J.; Nagase, S.; Kobori, Y.; Hasegawa, T.; Motomiya, K.; Tohji, K.; Kasuya, A.; Wang, D.; Yu, D.; Gao, Z.; Han, R.; Ye, H. *Chem. Mater.* **2006**, *18*, 4205.
(5) Maeda, Y.; Saito, K.; Akamatsu, N.; Chiba, Y.; Ohno, S.; Okui, Y.; Yamada, M.; Hasegawa, T.; Kako, M.; Akasaka, T. *J. Am. Chem. Soc.* **2012**, *134*, 18101.
(6) Pierce, A. E. *Silylation of Organic Compounds. A Technique for Gas Phase Analysis*; Pierce Chemical Company: Rockford, IL, 1968.
(7) Hof, F.; Bosch, S.; Eigler, S.; Hauke, F.; Hirsch, A. *J. Am. Chem. Soc.* **2013**, *135*, 18385.
(8) Hof, F.; Bosch, S.; Englert, J. M.; Hauke, F.; Hirsch, A. *Angew. Chem., Int. Ed.* **2012**, *51*, 11727.
(9) Englert, J. M.; Vecera, P.; Knirsch, K. C.; Schäfer, R. A.; Hauke, F.; Hirsch, A. *ACS Nano* **2013**, *7*, 5472.
(10) Eigler, S.; Hof, F.; Enzelberger-Heim, M.; Grimm, S.; Müller, P.; Hirsch, A. *J. Phys. Chem. C* **2014**, *118*, 7698.
(11) Hof, F.; Schäfer, R. A.; Weiss, C.; Hauke, F.; Hirsch, A. *Chem. - Eur. J.* **2014**, *20*, 16644.
(12) Milner, E. M.; Skipper, N. T.; Howard, C. A.; Shaffer, M. S. P.; Buckley, D. J.; Rahnejat, K. A.; Cullen, P. L.; Heenan, R. K.; Lindner, P.; Schweins, R. *J. Am. Chem. Soc.* **2012**, *134*, 8302.
(13) Fredenhagen, K.; Suck, H. *Z. Anorg. Allg. Chem.* **1929**, *178*, 353.
(14) Rüdorff, W.; Schulze, E. *Z. Anorg. Allg. Chem.* **1954**, *277*, 156.
(15) Catheline, A.; Valles, C.; Drummond, C.; Ortolani, L.; Morandi, V.; Marcaccio, M.; Iurlo, M.; Paolucci, F.; Penicaud, A. *Chem. Commun.* **2011**, *47*, 5470.
(16) Knirsch, K. C.; Englert, J. M.; Dotzer, C.; Hauke, F.; Hirsch, A. *Chem. Commun.* **2013**, *49*, 10811.
(17) Dye, J. L. *J. Phys. Chem.* **1980**, *84*, 1084.
(18) Malard, L. M.; Pimenta, M. A.; Dresselhaus, G.; Dresselhaus, M. S. *Phys. Rep.* **2009**, *473*, 51.
(19) Niyogi, S.; Bekyarova, E.; Itkis, M. E.; Zhang, H.; Shepperd, K.; Hicks, J.; Sprinkle, M.; Berger, C.; Lau, C. N.; deHeer, W. A.; Conrad, E. H.; Haddon, R. C. *Nano Lett.* **2010**, *10*, 4061.
(20) Englert, J. M.; Knirsch, K. C.; Dotzer, C.; Butz, B.; Hauke, F.; Spiecker, E.; Hirsch, A. *Chem. Commun.* **2012**, *48*, 5025.
(21) Strano, M. S.; Dyke, C. A.; Usrey, M. L.; Barone, P. W.; Allen, M. J.; Shan, H.; Kittrell, C.; Hauge, R. H.; Tour, J. M.; Smalley, R. E. *Science* **2003**, *301*, 1519.
(22) Usrey, M. L.; Lippmann, E. S.; Strano, M. S. *J. Am. Chem. Soc.* **2005**, *127*, 16129.
(23) Chattopadhyay, J.; Chakraborty, S.; Mukherjee, A.; Wang, R.; Engel, P. S.; Billups, W. E. *J. Phys. Chem. C* **2007**, *111*, 17928.
(24) Schmidt, G.; Gallon, S.; Esnouf, S.; Bourgoin, J.-P.; Chenevier, P. *Chem. - Eur. J.* **2009**, *15*, 2101.
(25) Ramirez, J.; Mayo, M. L.; Kilina, S.; Tretiak, S. *Chem. Phys.* **2013**, *413*, 89.
(26) Vecera, P.; Holzwarth, J.; Edelthalhammer, K. F.; Mundloch, U.; Peterlik, H.; Hauke, F.; Hirsch, A. *Nat. Commun.* **2016**, *7*, 12411.
(27) Graf, D.; Molitor, F.; Ensslin, K.; Stampfer, C.; Jungen, A.; Hierold, C.; Wirtz, L. *Nano Lett.* **2007**, *7*, 238.
(28) Challet, S.; Azaïs, P.; Pellenq, R. J. M.; Isnard, O.; Soubeyroux, J. L.; Duclaux, L. *J. Phys. Chem. Solids* **2004**, *65*, 541.
(29) Rauf, H.; Pichler, T.; Knupfer, M.; Fink, J.; Kataura, H. *Phys. Rev. Lett.* **2004**, *93*, 096805.
(30) Syrgiannis, Z.; Gebhardt, B.; Dotzer, C.; Hauke, F.; Graupner, R.; Hirsch, A. *Angew. Chem., Int. Ed.* **2010**, *49*, 3322.
(31) Hirsch, A.; Brettreich, M. *Fullerenes: Chemistry and Reactions*; Wiley-VCH: Weinheim, Germany, 2004.
(32) Knirsch, K. C.; Schäfer, R. A.; Hauke, F.; Hirsch, A. *Angew. Chem., Int. Ed.* **2016**, *55*, 5861.

DOI: 10.1021/jacs.6b09487
J. Am. Chem. Soc. 2016, 138, 15642−15647